Surface phenomena and protective film growth on magnesium and magnesium alloys

Sachiko Ono*
Advanced Research Institute for Science and Engineering, Waseda University, Shinjuku-ku, Tokyo 169, Japan.

Abstract

Recent research development concerning the filming behavior of magnesium and magnesium alloys is reviewed. The naturally formed film on magnesium in air is thin and dense, and it has an amorphous structure. In humid air, a hydrated layer forms between the metal and initial layer as a result of water ingress through the initial layer. The film formed in water contains an additional top layer with platelet-like morphology, formed by re-deposition of sparingly soluble magnesium. With increasing aluminum content of the alloys, all layers became dehydrated and enriched in aluminum oxide, and they decrease in thickness. These changes are significant especially as the aluminum content of the alloy is increased above 4 wt %, a threshold characterized also by a significant improvement in the corrosion resistance. This transition, corresponds to 35 wt % of Al in the innermost layer of the oxide film. Alloying of the MgAl alloys with rare earth elements, causes further improvement of the corrosion resistance. This is attributed to a significant dehydration, causing increased stability and passivity of the oxide. For the anodic film growth on pure magnesium, the cylindrical pore structure and barrier layer which are similar to the Keller's model of anodic alumina are confirmed by direct cross- sectional observation. It is assumed that anodic film growth proceeds mainly by the formation of MgF_2 and $Mg_{x+y/2}O_x(OH)_y$ at the metal/film interface and the dissolution of the film at pore bases. The crystallization of MgF_2 and the formation of $NaMgF_3$ simultaneously proceed in the porous layer. The similar pore structure is also found in the film grown on magnesium die cast AZ91D, however, the film is highly uneven in thickness. The film surface after chemical conversion coating has a granular structure, with each granule corresponding to a single grain. It was revealed that the film was formed by anodic reaction and had a porous cell structure. The porous film is composed of cell colonies in the sub-micron range that have branched fine pores, with central holes (mother pores) sized approximately 50 nm. Square shaped holes about 300 nm in size are believed to be cathodic sites.

Riassunto

Vengono prese in considerazione le più recenti ricerche sulla formazione degli strati sottili (ovvero film) superficiali sulle leghe di alluminio e di magnesio. Il film che naturalmente si forma sul magnesio è sottile e denso e di struttura amorfa. Se l'aria è umida, tra il metallo e lo strato primario viene a formarsi uno strato idratato a causa della penetrazione dell'acqua attraverso lo strato primario. Il film che si forma nell'acqua comprende uno strato superiore supplementare simile morfologicamente a piastrine create dalla rideposizione di magnesio scarsamente solubile. Man mano che aumenta nelle leghe il titolo d'alluminio tutti gli strati diventano disidrati, si arrichiscono di ossido di alluminio e si assottigliano. Queste alterazioni sono importanti, particolarmente in quanto il titolo della lega in alluminio viene portato al di sopra del 4% per peso, soglia, questa, caratterizzata da un miglioramento significativo della resistenza alla corrosione. Detta transizione corrisponde al 35% per peso dell'Al nello strato più interno del film ossidato.

L'alligazione delle leghe MgAl con gli elementi del gruppo delle terre rare porta ad un ulteriore miglioramento della resistenza alla corrosione che si pensa sia dovuto ad una disidratazione importante, la quale aumenta sia la stabilità sia la passività dell'ossido. Per quanto concerne la crescita del film anodico sul magnesio puro, la struttura dei pori cilindrici ed lo strato che funge da barriera sono simili a quelli del modello del Keller e sono stati confermati dalla osservazione diretta della sezione traversale. Si presume che la crescita del film anodico proceda in buona parte con la formazione del MgF_2 ed del $Mg_{x+y/2}O_x(OH)_y$ all'interfaccia metallo-film, nonché per la dissoluzione del film stesso alla base dei pori. Procedono contemporaneamente nello strato poroso la cristallizzazione del MgF_2 e la formazione del $NaMgF_3$. Una struttura porosa simile appare anche nel film che cresce sul magnesio AZ91D pressofuso, sebbene lo spessore del film stesso sia altamente irregolare. La superficie del film dopo il rivestimento per conversione chimica presenta una struttura granulare nella quale ogni granulo corrisponde ad un unico grano. E' stato dimostrato che il film in parola si è formato a causa di una reazione anodica e che è dotato di una struttura cellulare porosa. Il film poroso è composto da colonie di cellule submicrometriche con pori fini ramificati e pori centrali ("madri") di Ø 50 nm circa. Si ritiene che i pori quadri di 300 nm circa siano dei siti catodici.

INTRODUCTION

The practical importance of magnesium as a light metal, especially in the fields of automobile industry and welfare related commodities such as wheel chairs has remarkably increased. However, only limited information (1-4) on the surface phenomena and protective film growth on magnesium is available in contrast to the numerous investigations on the surface oxides on aluminum. This is partly due to difficulties in dealing with the surface of magnesium because of its high reactivity.

Significant improvement in the corrosion resistance of cast MgAl alloys have been achieved during the past decade by reduction of the heavy metal impurity content, alloying, and

*Present address: Research Organization for Advanced Engineering, Shibaura Institute of Technology, Ohmiya-shi, Saitama 330-8570, Japan

heat-treatment. These advantages can be understood partly in terms of increased passivity of the metal surface by incorporation of components which stabilize the oxides. A fundamental study of corrosion-resistant oxides forming on magnesium alloys must be based on the knowledge of the structure and properties of oxides on pure magnesium, and how these properties are modified as a result of alloying. Therefore, morphology and structure of oxide films formed naturally in air and water were characterized, and it was investigated whether the properties of these oxide films were correlated with the corrosion behavior of MgAl alloys in aqueous media (5-9).

In addition to the investigation on the surface passivation phenomena, the formation behavior and the structure of surface films grown by anodizing and chemical conversion coating, which are most commonly used surface protective treatments of magnesium and its alloys, were studied. The oxide films formed by surface treatments significantly improve corrosion resistance of magnesium which is shown by corrosion tests in aqueous media and atmospheres. Recently, the cylindrical porous structure of the anodic films, which is comparable to the Keller's model of anodic alumina (10), and their fundamental growth mechanism are established, for the first time, by the direct cross sectional observation and surface characterization of the films(11,12). The authors also reported growth mechanism, microstructure and composition of surface films formed by chemical conversion coating on magnesium die cast AZ91D and pure magnesium (13-15).

The present paper reviews the above investigations concerning surface phenomena and oxide film growth which have been studied by using SEM, TEM combined with ultramicrotomy, XRD, EDX and XPS to clarify the growth mechanism for the better understanding of the surface nature of magnesium.

MORPHOLOGY AND STRUCTURE OF NATURALLY FORMED OXIDES IN AIR AND WATER

Naturally formed oxides on pure magnesium in air and water (5,6)

The initial film formed on pure Mg (99.99%) immediately after exposing freshly trimmed metal surface to air is thin (approximately 25 nm) and dense (continuous), and it has an amorphous structure as shown in Fig.1. In humid air, a hydrated layer forms between the metal and initial layer as a result of water ingress through the initial layer and metal oxidation. The hydrated layer can be visualized as a result of dehydration process induced by sustained exposure of the oxide to the electron beam of TEM, giving the layer of a cellular appearance as indicated in Fig.2. The film formed in water contains an additional top layer with platelet-like morphology, formed by re-deposition of sparingly soluble magnesium, which migrates outward also through the initial layer. TEM image of this three layered oxide morphology, consisting of the innermost hydrated layer, the intermediate dense layer and the outermost platelet layer is shown in Fig.3.

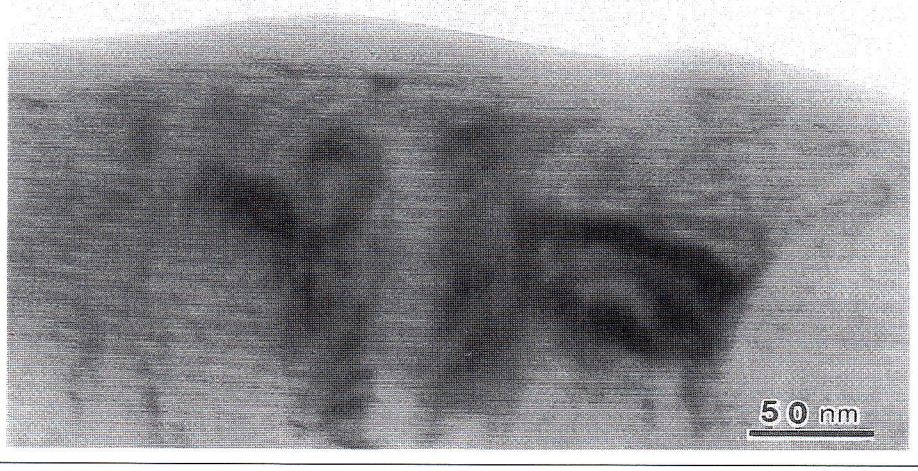

Figure 1: TEM image od an ultramicromed cross section of the film formed on pure magnesium in air showing a dense and amorphous layer

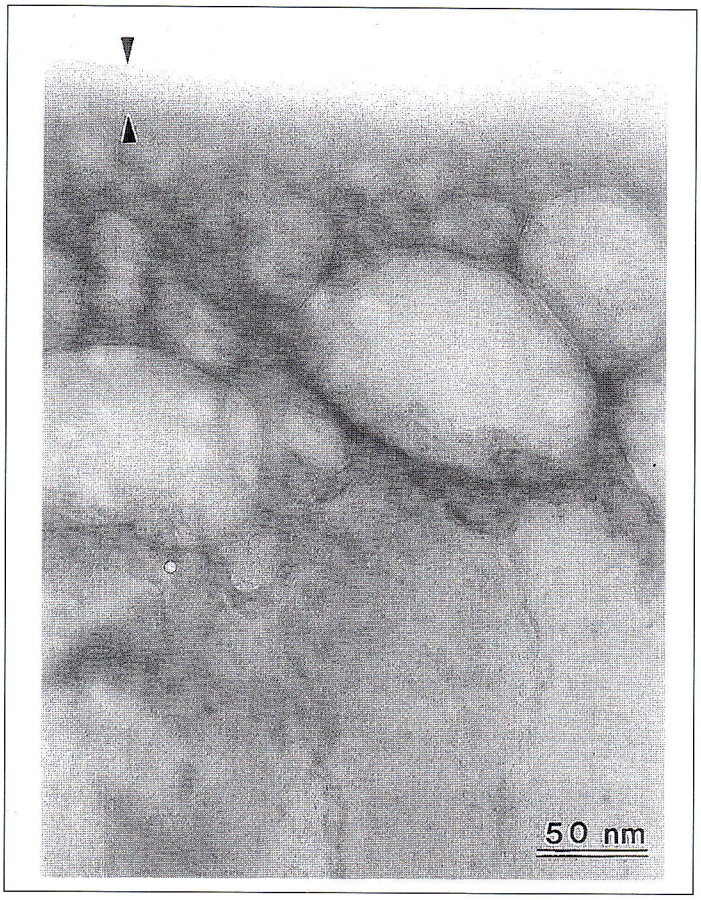

Figure 2: TEM image of an ultramicrotomed cross section of the film formed on pure magnesium after exposure in humid environment, showing a duplex structure with a dense amorphous outer layer (black arrows) and an electron beam sensitive inner layer

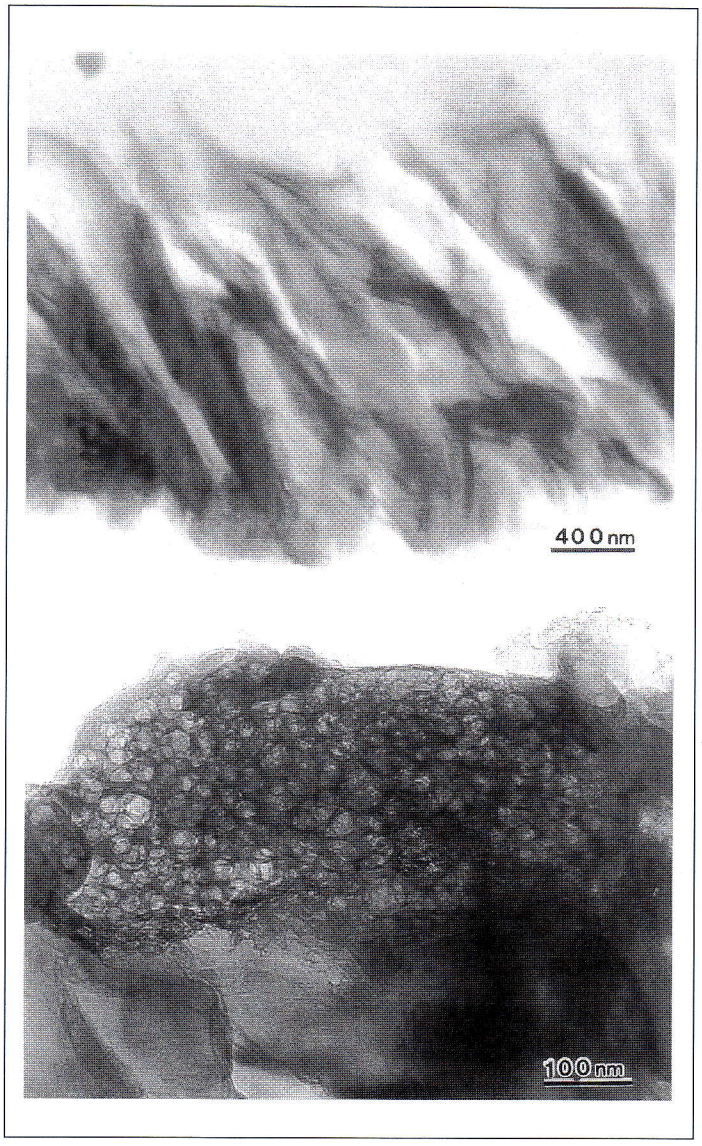

Figure 3: TEM image of an ultramicrotomed cross section of the film formed on pure on magnesium after immersion in water for 48 h showing three layered oxide, consisting of the innermost hydrated layer, the intermediate dense layer and the outermost platelet layer

Naturally formed oxides on MgAl alloys in air and water (7)

The initial air-formed films on MgAl alloys are amorphous and dense similarly to the film formed on pure magnesium. Composition of the investigated materials obtained by spectrographic analysis is listed in Table 1. Typical bright and dark field TEM images of the film section are shown in Fig.4. As clearly seen in Fig.5, a significant reduction in the film thickness occurred when Al content in the alloy was increased to 5%, while further alloying with aluminum resulted in minor changes. In addition to thickness measured from TEM images, limiting thickness estimated from earlier XPS data (16) by use of Cabrera-Mott kinetics are included for comparison. In view of similarities between TEM data and earlier XPS data, it is deduced that the air formed film is formed by a field-assisted cation transport mechanism described by the Cabrera-Mott theory (17). With reference to the XPS data, this corresponds to an aluminum concentration of about 35% in the oxide.

Table 1 - Composition of the investigated materials obtained by spectrographic analysis

Alloy	Al	Mn	Zn	Si	Fe	Cu	Ni
Mg (99.99%)	-	-	-	-	-	-	-
AM 20	2.0	0.50	0.01	0.01	0.002	0.001	0.0005
Mg 3% Al	3.1	-	-	-	-	-	-
AM 50	5.0	0.26	0.01	0.01	0.002	0.002	0.0006
AM 60	5.8	0.26	0.01	0.02	0.0064	0.002	0.0005
AM 80	8.0	0.26	0.01	0.01	0.004	0.002	0.0008

The film formed in water also exhibits the three-layered structure found on pure magnesium. TEM image of the film section formed on AM80 is shown in Fig.6. With increasing aluminum content of the alloys, all layers became dehydrated and enriched in aluminum oxide, and they decrease in thickness (Fig.7). The change in thickness is most dramatic for the platelet layer and least significant for the intermediate layer. These changes are significant especially as the aluminum content of the alloy is increased above 4 wt %, a threshold characterized also by a significant improvement in the corrosion resistance. This transition, which corresponds to 35 wt % of Al in the innermost layer of the oxide film, is determined by EDX point analysis of the oxide cross section (Figs.8 and 9). The alumina component of the inner layer is becoming the dominating factor in determining the passivity of the surface, presumably by forming a continuous skeletal structure in an amorphous mixture of aluminum and magnesium (hydr-)oxides. This value agree well with the composition of oxides grown on the same type of alloys in ultra-high vacuum and dry air (16). The innermost layer is responsible for the passivity of the surface in the presence of an aqueous environment. The original air-formed film

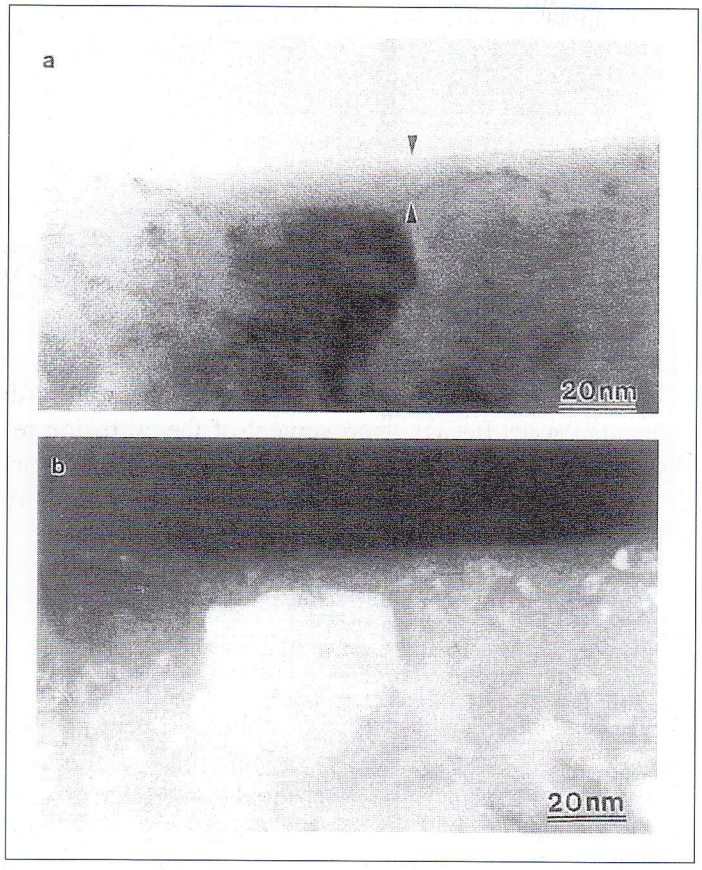

Figure 4: Typical (a) bright and (b) dark field TEM images of the film formed on MGAl (AM60) alloy

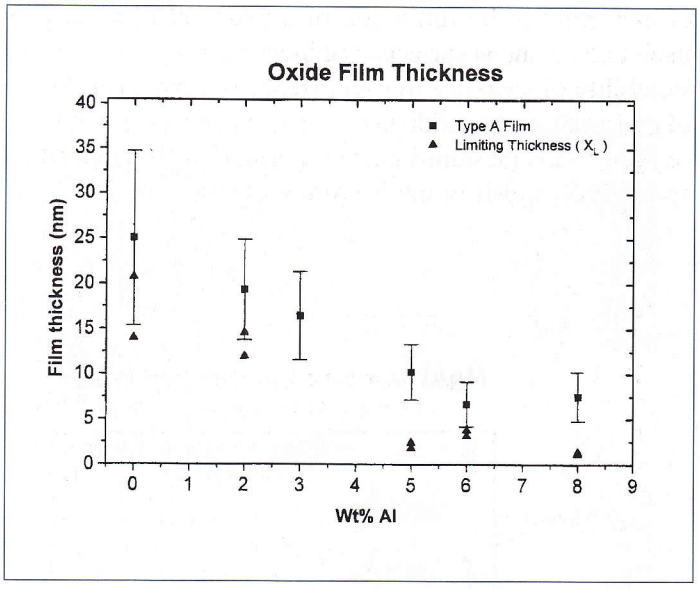

Figure 5: Thickness of air formed film as a function of Al content in the alloy. Limiting thickness data estimated from earlier XPS measurements are also included for comparison (16)

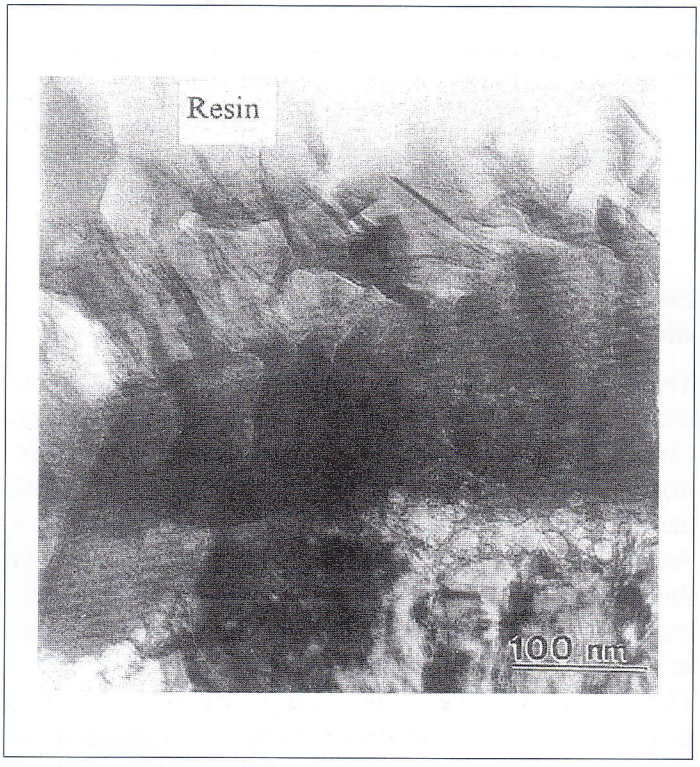

Figure 6: Cross section of the film formed on AM80 after immersion in water for 48h

cannot prevent the formation of a hydrated film between itself and the metal surface. The innermost layer reflects the instability of the oxide in the presence of water. The degree of hydration of the oxide layers is deduced from the ratio of oxygen to magnesium intensity peaks (I_0/I_{Mg}) obtained by spot EDX analysis of oxide cross sections.

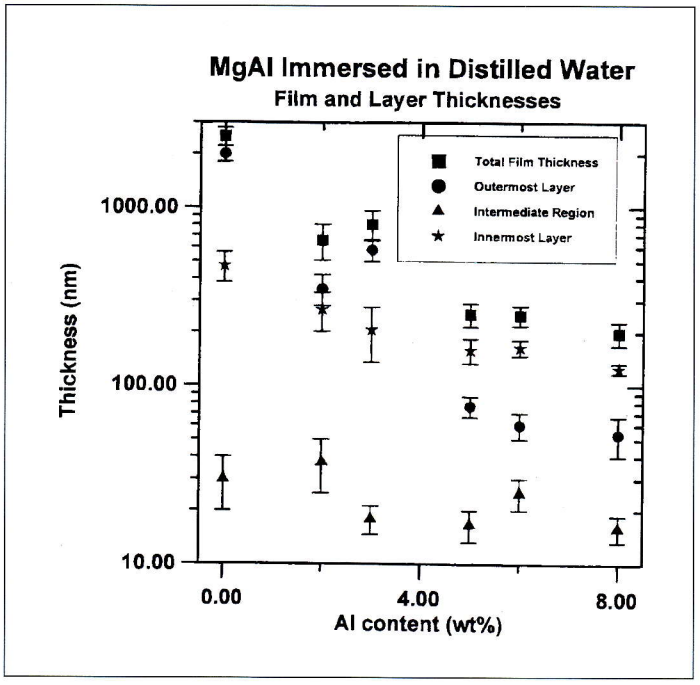

Figure 7: Total film thickness and layer thickness of water formed film as a function of Al content of the alloy

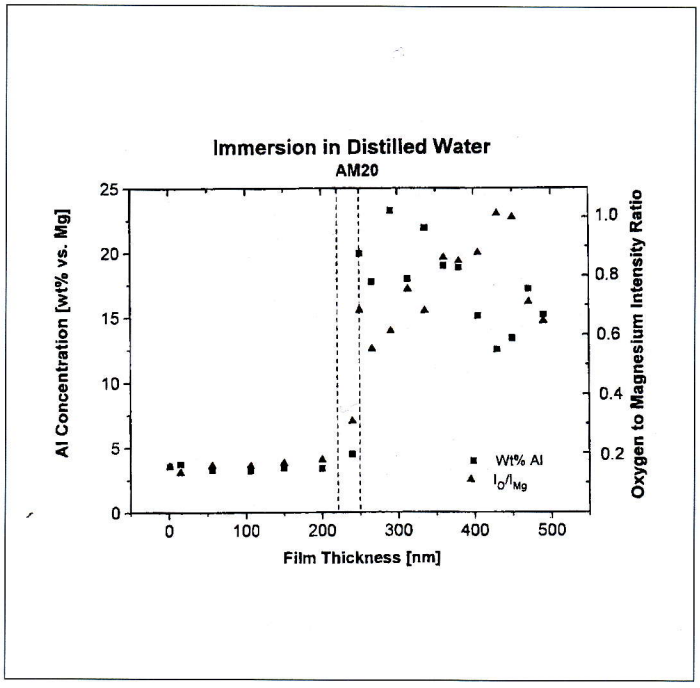

Figure 8: Aluminum concentration and oxygen-to-magnesium peak intensity depth profiles of oxide film on an AM 20 specim obtained by EDX point analysis. Dashed lines mark the layer interfaces

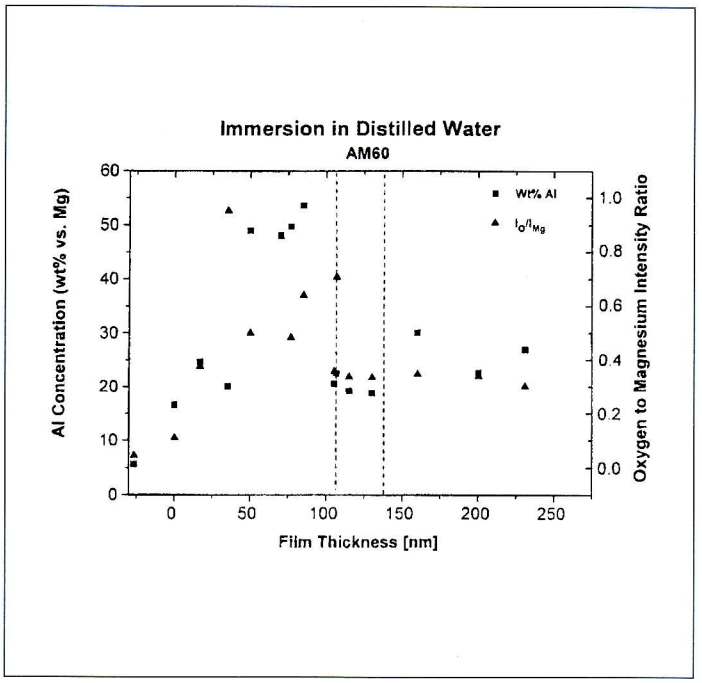

Figure 9: Aluminum concentration and oxygen-to-magnesium peak intensity depth profiles of oxide film on an AM 60 specim obtained by EDX point analysis

Alloying of the MgAl alloys, in addition, with rare earth elements causes further improvement of the corrosion resistance. This is attributed to a significant dehydration, particularly of the innermost layer, causing increased stability and passivity of the oxide.

Water-Formed Oxides on Ternary MgAl Alloys (8)

Oxides on ternary magnesium alloys MgAlZn and MgAlRE were investigated by TEM using ultramicrotomed film sections. These films have a three- layered structure, similar to pure Mg and binary MgAl alloys, characterized by a hydrated inner layer, a thin and dense intermediate region, and a platelet-like outer layer. Zinc and rare-earth elements present in the two types of ternary alloys became incorporated in the oxide film so as to increase its stability in an aqueous environment, in particular by reducing hydration and increasing resistance to magnesium egress of the inner layer, which is responsible for the passivity of the surface. The apparent presence of trace amount of rare-earth oxides in the film is particularly effective in improving passivity of the surface and, thereby, the corrosion resistance of MgAlRE alloys. The presence of aluminum together with rare-earth elements (RE) in the alloy is an essential factor in obtaining these results.

COMPOSITION, STRUCTURE AND GROWTH MECHANISM OF ANODIC FILMS

Anodic film growth on pure magnesium (11)

Anodic films were formed on pure (99.6%) magnesium sheets at 200 Am^{-2} up to 70 V for 2 min in a solution containing 300 g of NH_4HF_2, 100 g of $Na_2Cr_2O_7$ and 90 ml of H_3PO_4 (Dow 17, a product of Dow Chemical Co., which is a most commonly used electrolyte for anodization of magnesium) at 70°C. The sparking accompanied by the electric breakdown was not detected during the film growth. The cross sections of the films were prepared by ultramicrotomy using a diamond knife, in the thickness range of 20 to 50 nm (18). Specimens were embedded in a resin before the sectioning.

As shown in Fig. 10, cylindrical pore structure and barrier layer (see the arrow) in contact with metal substrate, which are similar to the Keller's model of anodic films on aluminum, are evident. The metal substrate is partly hydrated

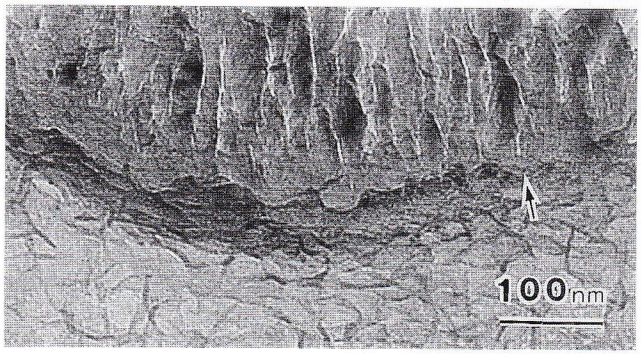

Figure 10: TEM image of an ultramicrotomed cross section of the anodic film formed at 70°C on pure magmesium at 200 Am^{-2} up to 70 V for 2 min in Dow 17. Arrow sign shows the barrier layer connected to the metal substrate under the cylindrical pore.

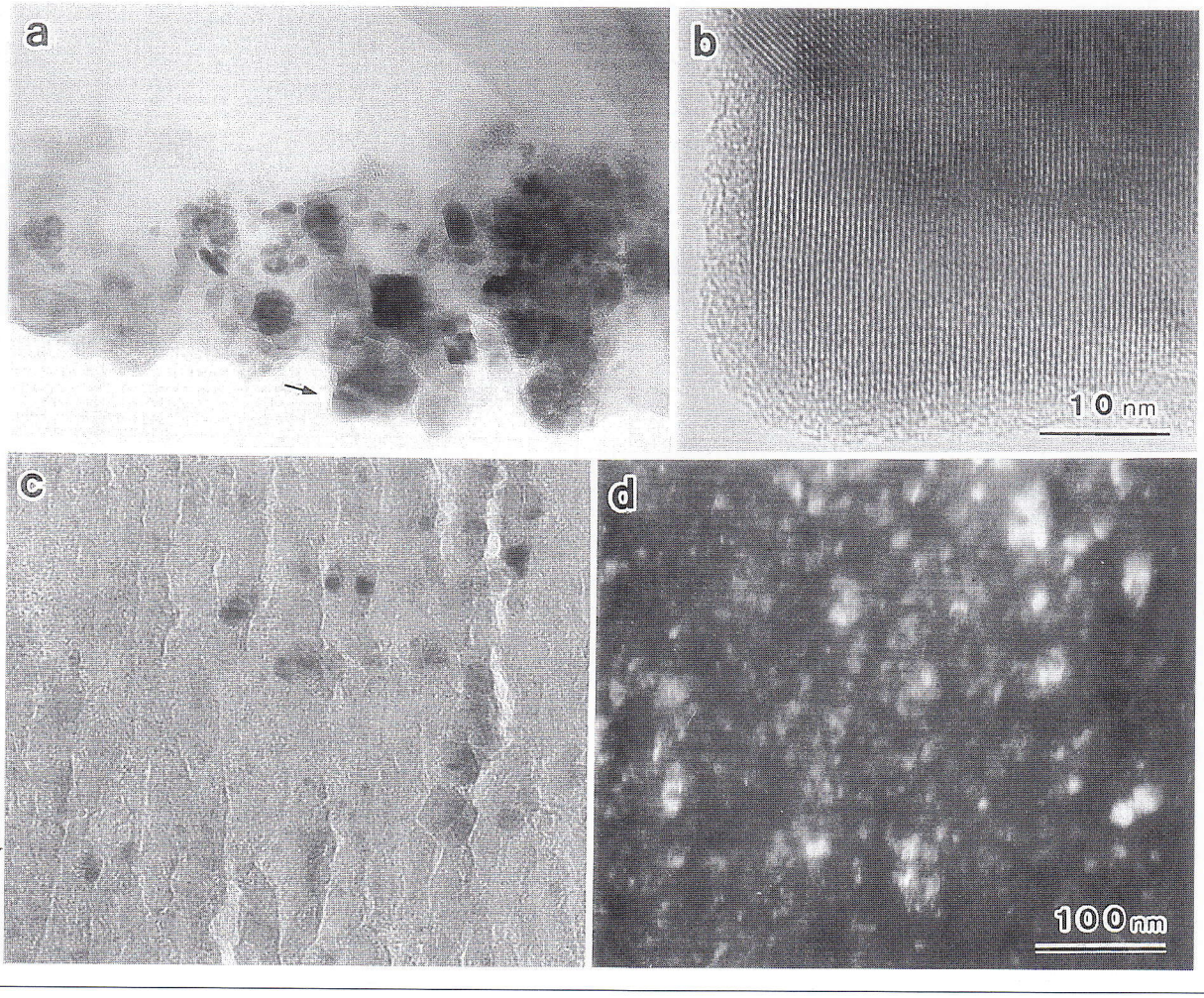

Figure 11: TEM image of an ultramicrotomed cross section of the anodic film on pure magmesium. (a) The outermost part of the film showing a number of crystalline particles. This part embedded in a resin was separated from the bulk of the film during the sectioning. (b) High resolution image of the crystal indicated by the arrow sign in (a) shows lattice fringes of MgF^2. (c) Bright field and (d) dark field images of the middle part of the film showing dispersed crystals. a, c, d: Same magnification.

during the sectioning to exhibit a platelet feature. Cell diameter (15 nm) and barrier layer thickness (10 nm) formed at 70 V are found to be notably smaller than those associated with anodic alumina (19). The electric field strength across the barrier is as high as 10^{10} Vm^{-1}. The presence of the barrier layer under the bulk porous film was presumed by Bradford et al. (20) and Gulbrandsen et al. (21) in the investigations of the passivation behavior of magnesium by using electrochemical methods. Recently, some of the present authors found that the porous film formed on magnesium die cast by chemical conversion coating was also separated from the substrate by thin barrier layer at the metal / film interface (13,14).

In the outermost part of the film (Fig. 11a) having a number of crystalline particles, the regular pore structure was lost because of the film dissolution in the electrolyte. Bright field and dark field images of the middle part of the film (Fig. 11c, d) exhibit dispersed crystalline particles with the size up to 40 nm in the amorphous matrix. The size and the number of crystals appear to increase in the outer part of the film. They were identified as MgF_2, and $NaMgF_3$, by electron diffraction patterns, which were obtained from the middle and the outer part of the film. Only MgF_2, was found in the vicinity of the film / substrate interface. X-ray diffraction analysis supports the presence of crystalline MgF_2, and $NaMgF_3$, in the film (2,3,4).

Since the thickness of the film is approximately 5.5 μm, the current efficiency for the film formation is calculated to be about 400%, if the film is postulated to be composed of MgO and if the metal substrate is assumed to dissolve as Mg^{2+}. This result suggests complex reactions for anodic film growth on magnesium compared with the growth of anodic alumina films. In the latter case, the efficiency is nearly 100% when Al_2O_3 is postulated for the film composition. The apparent high current efficiency may be partly caused by the incorporation of solution species from the electrolyte into the film in addition to the products of usual electrochemical reactions.

XPS quantitative analysis was performed by considering the integrated spectral intensities and photo ionization cross sections (22,23). The results indicate that the film contains large amounts of F^- and Mg^{2+}, medium amounts of Na^+, O^{2-} and OH^- and small amounts of P^{5+}, Cr^{3+} and NH_4^+. Since MgO crystal is hardly found in the film by the electron diffraction, it will be amorphous magnesium oxyhydroxide that is formed. Considering the electron binding energies and Auger parameters, the film constituents are likely to be MgF_2, $Mg_{x+y/2}O_x(OH)_y$, PO_4^{3-}, Cr_2O_3 and NH_4^+ as listed in Table 2 with their molar ratios. If the values in Table 2 are taken into account, the current efficiency of the film formation obtained by rough estimation becomes approximately 230%. Based on the above results, the following process of anodic film growth on magnesium can be deduced. Anodic film growth proceeds mainly by the formation of MgF_2 and $Mg_{x+y/2}O_x(OH)_y$ (magnesium oxyhydroxide) at the metal / film interface and the dissolution of the film at pore bases. The mobility of F^- across the barrier layer may be higher than that of O^{2-}. MgF_2 crystallizes in the amorphous $Mg_{x+y/2}O_x(OH)_y$ matrix after transfer from the barrier layer to the porous layer, resulting in an escape from the high electric field. $NaMgF_3$ is formed along with film growth in the middle part of the film by a chemical reaction under the presence of Na^+ in the electrolyte. The formation and incorporation of Cr_2O_3 in the film can occur as a result of the reduction of Cr^{6+} to Cr^{3+} at the counter electrode.

Table 2 - XPS quantitative analysis of the anodic film on pure magnesium. Compounds are identified from the electron binding energies and Auger parameters, and their mole% was estimated from atomic % of individual elements

Element	wt%	at%	Compound	mole %
Mg	31.75	27.16	MgF_2	31
Na	11.61	10.50	$NaMgF_3$	37
Cr	1.51	0.60	Cr_2O_3	1
P	1.10	0.74	PO_4^{3-}	2
F	45.53	49.83	-	-
N	0.63	0.94	NH_4^+	3
O	7.88	10.24	$Mg_{x+y/2}O_x(OH)_y$	26

Anodic film growth on magnesium die cast AZ91D (12)

The structure and the growth mechanism of anodic oxide films grown on magnesium die cast AZ91D were then studied by electron microscopy combined with an ultramicrotomy technique. Table 3 shows chemical composition of magnesium die cast (AZ91D). As shown in SEM images of surfaces after anodizing in Dow 17 (Fig. 12) and a cross section embedded in a resin (Fig. 13), the anodic films are highly uneven in thickness. This may have been caused by film destruction resulting from breakdown accompanied by gas evolution, and also by uneven anodic reaction owing to the presence of cavities and compositional irregularities at the grain boundaries. Bright field and dark field images of the film (Fig. 14) exhibit dispersed crystalline particles with the size up to 40 nm. Table 4 indicates lattice spacings obtained from electron diffraction patterns of the anodic film compared with ASTM standards. Porous cell structure with dispersed MgF_2 and $NaMgF_3$ crystalline particles is found in the films. It is assumed that anodic film growth proceeds by the formation of MgF_2 and magnesium oxyhydroxide at the metal/film interface and the dissolution of the film at the pore bases. The crystallization of MgF_2 and the formation of $NaMgF_3$ subsequently proceed in the porous layer.

The film growth mechanism of magnesium under anodization is rather complicated in comparison with that of aluminum. The direct cross sectional observation by TEM combined with ultramicrotomy technique and XPS surface characterization yielded useful results to establish the growth mechanism of surface films on magnesium; however, further information is needed for more complete clarification of the mechanism.

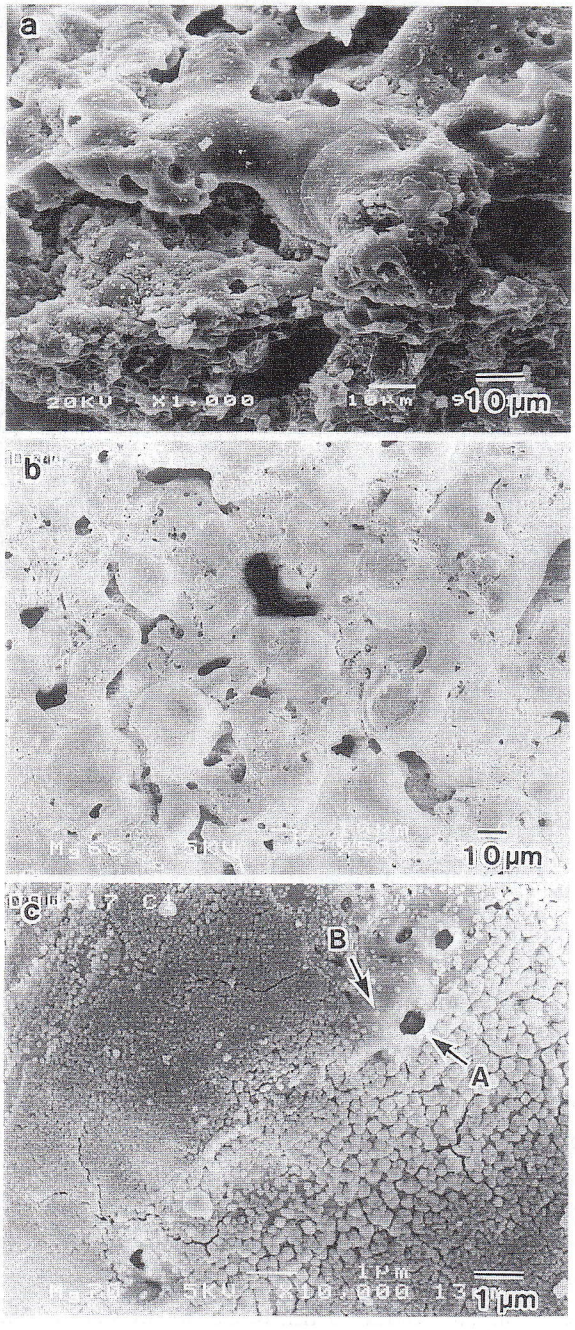

Figure 12: SEM image of surfaces of AZ91D after anodizing in Dow 17. (a) shows both top and fracture surfaces at different magnifications

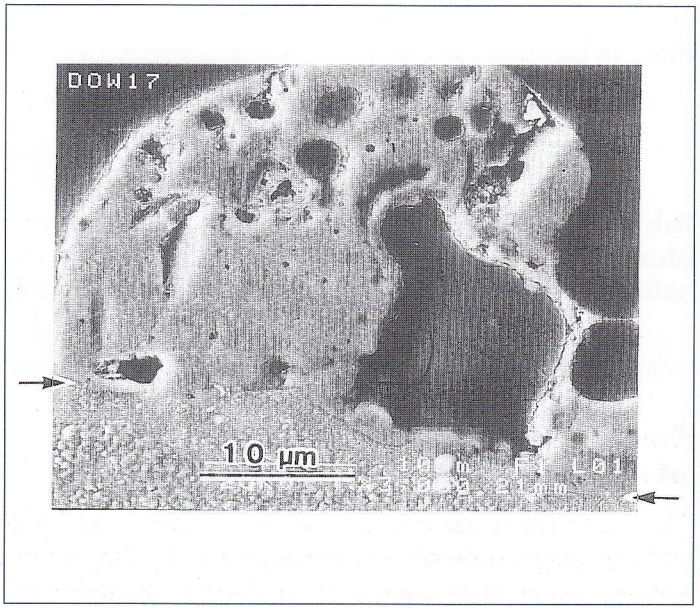

Figure 13: SEM image of a cross section of the anodic film formed on AZ91D in Dow 17 and embedded in a resin. Arrows indicate film/substrate interface

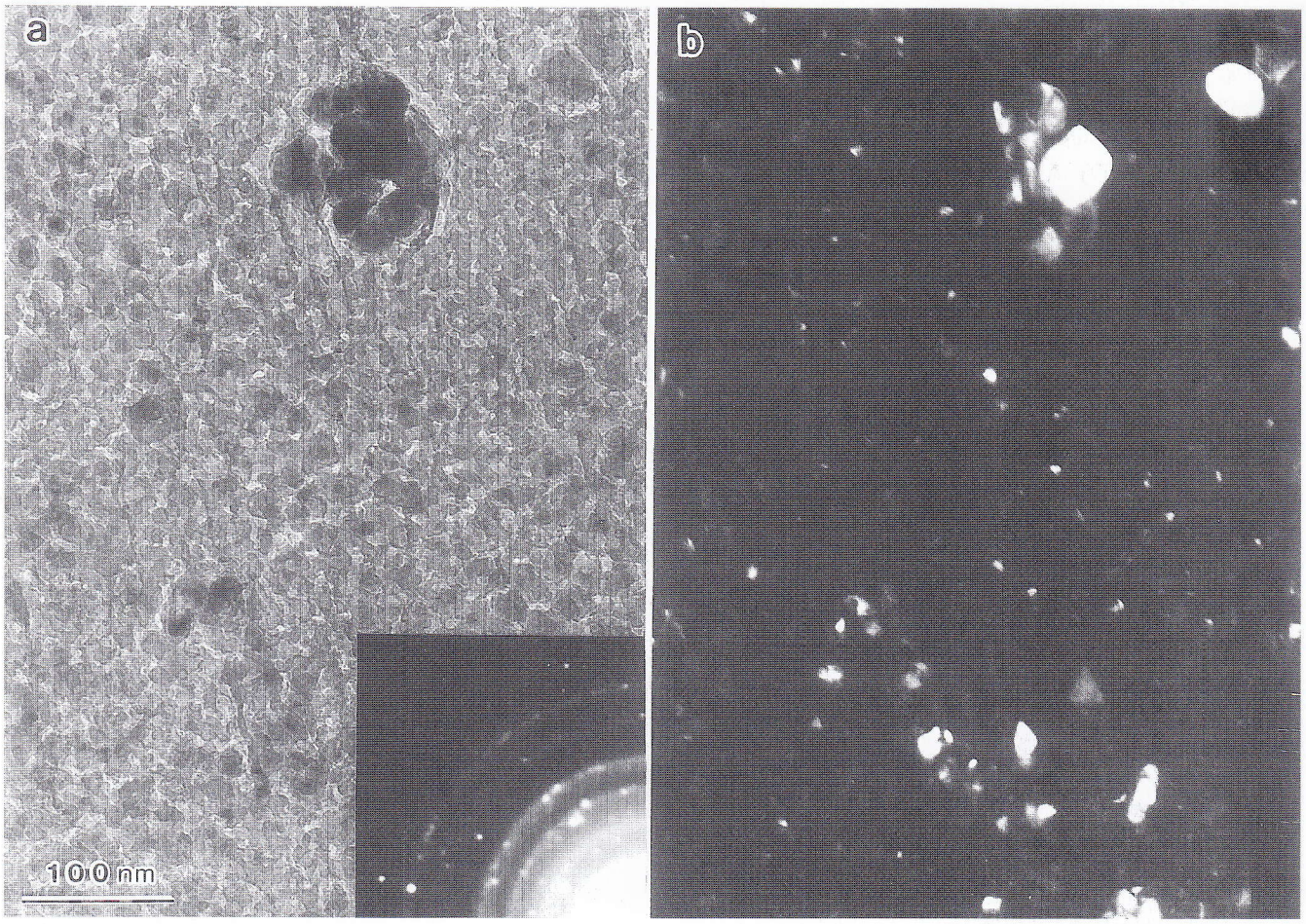

Figure 14: TEM images of an ultramicrotomed cross section and diffraction pattern of the anodic film on AZ91D. a: bright field image. b: dark field image

COMPOSITION, STRUCTURE AND FORMATION MECHANISM OF CHEMICAL CONVERSION COATING FILMS

Surface morphology and microstructure observed by SEM (13)

The magnesium die cast AZ91D (see Table 3) and pure (99.6%) magnesium sheets were degreased by dipping in a commercial alkaline solution at 70°C for 5 min and subsequently etched in a solution containing 300 gdm^{-3} of NH_4HF_2 at room temperature for 5 min. Conversion coating films, which are also called as chromate films, were formed by immersions in a solution containing 150 gdm^{-3} of $Na_2Cr_2O_7$ and 2.5 gdm^{-3} of MgF_2 (Dow 7, a product of Dow Chemical Co., which is a most commonly used electrolyte for chemical conversion coating of magnesium) at 95°C for 10 min for AZ91D and 30 min for pure Mg. SEM images of a surface of the chemical conversion coating (Dow 7) on Magnesium die cast AZ91D were shown in Fig. 15 as well as AFM image in Fig.16. The film has a granular structure, with each granule corresponding to a single grain in the size of 2 µm to 7 µm. Typically, large (Arrow A in Fig.15) and small (Arrow B in Fig.15) holes about 300 nm and 50 nm in size are observed on a grain. High resolution images revealed fine particles approximately 5 nm to 20 nm in size on the film surface. Cavities deeply penetrated into the substrate at grain boundaries are also observed. Large numbers of cracks which are thought to be originated in the grain structure of the

substrate are shown on the surface of the film grown on pure magnesium. Namely, grain boundaries are suggested to act as cathodic sites and to be passages of evolved hydrogen. Large and small holes about 300 nm and 50 nm in size respectively, and fine particles on the surface are also detected in the film on pure magnesium.

Table 3 - Chemical composition of magnesium die cast AZ91D

Element	Al	Zn	Mn	Be	Si	Cu	Ni	Fe	Cl
mass %	9.0	0.7	0.24	0.0002	0.02	0.005	0.0005	0.001	0.002

Table 4 - Lattice spacings obtained from electron diffraction patterns of the anodic film on magnesium die cast AZ91D compared with ASTM standards (unit: 0.1 x nm)

Anodic film	2.71	2.06	1.92	1.72	1.55	1.43	1.30	1.25
MgF_2	-	2.07	-	1.71	1.52	1.38	1.32	1.23
$NaMgF_3$	2.76	-	1.92	1.71	1.56	1.36	1.30	-

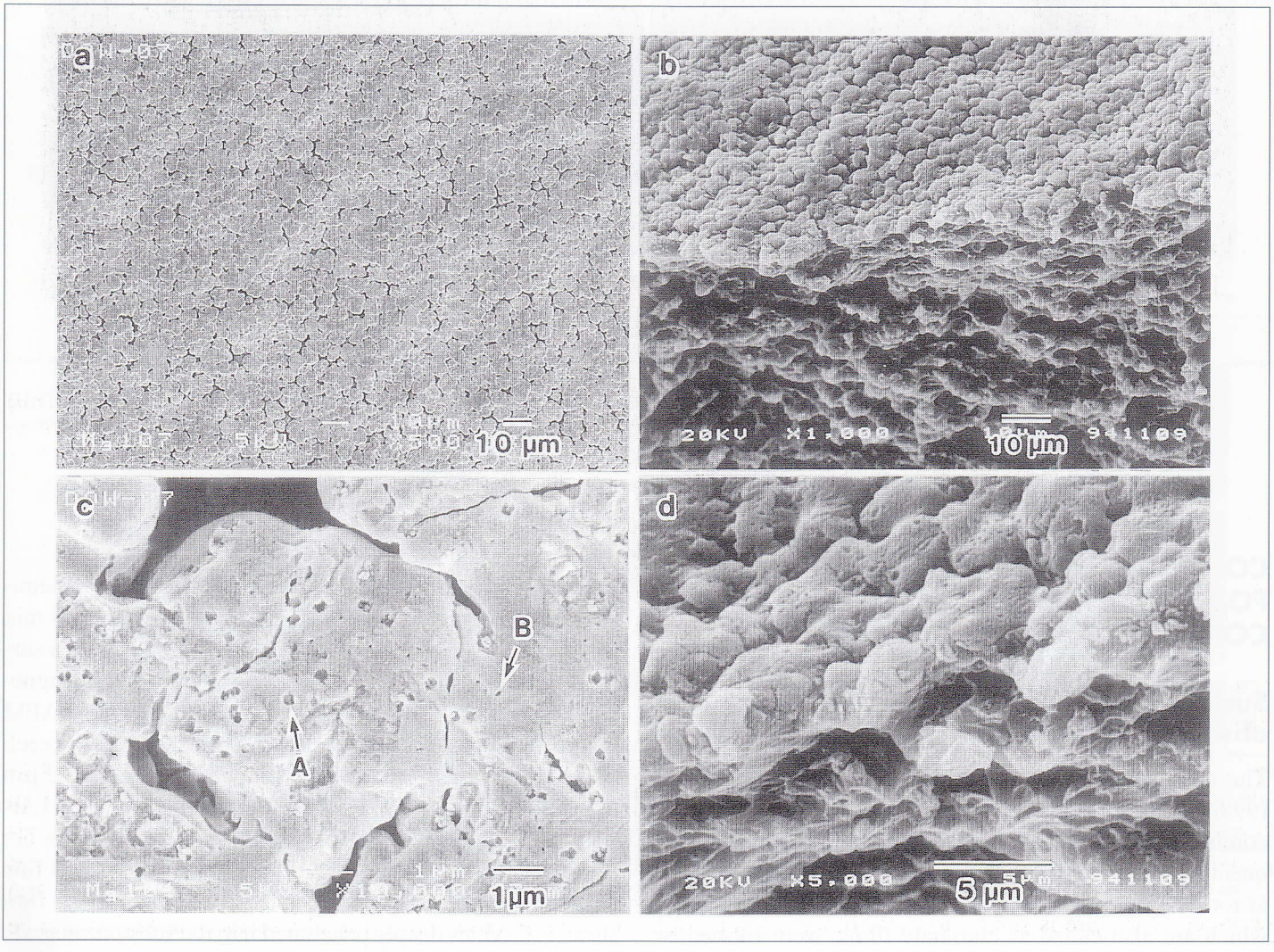

Figure 15: SEM images of surfaces of AZ91D after chemical conversion (chromate) coating in Dow 7. (b) and (d) both top and fracture surfaces at different magnifications

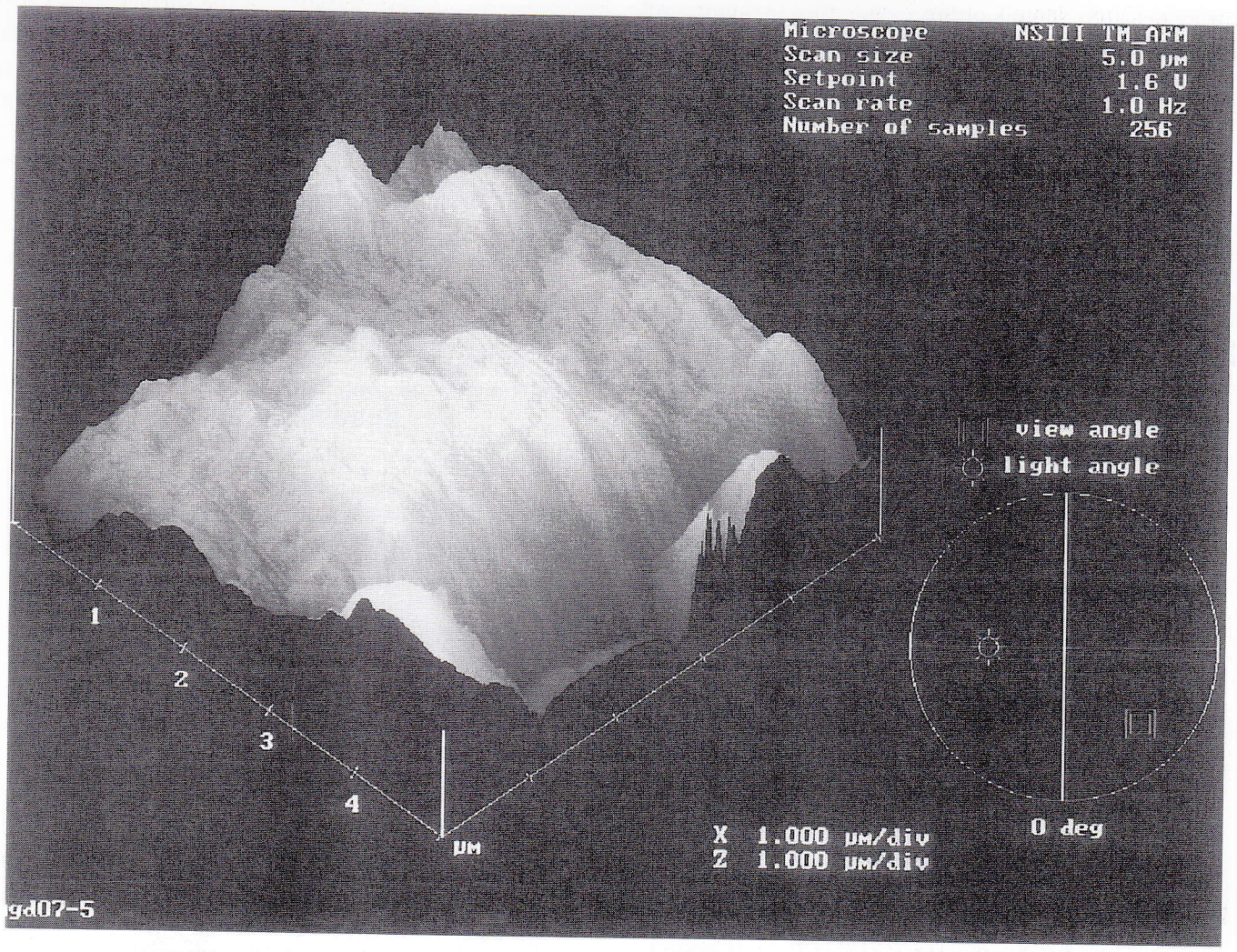

Figure 16: AFM image of the surface of AZ91D after chemical conversion coating

Ultramicrotomed cross sections observed by TEM (13)

As shown in Fig. 17, the bright field image of the ultramicrotomed cross section of the film formed on AZ91D reveals that the film is grown by anodic reaction and has a porous cell structure which is separated from the substrate by a thin barrier layer at the film/metal interface. This cylindrical cell structure is similar to those observed in anodic films (11,12), though the diameter of pores (5 nm) and barrier layer thickness (5 nm) are rather small. The porous film is suggested to be composed of cell colonies in the sub-micron range that branching into fine pores, with central holes (mother pores) sized approximately 50 nm. Holes about 300 nm in size observed on the film surface are believed to be

cathodic sites and are made by hydrogen evolution. Schematic model of the chemical conversion film including cell colonies and mother pores is shown in Fig.18. The film appeared to be amorphous, however, small crystalline particle

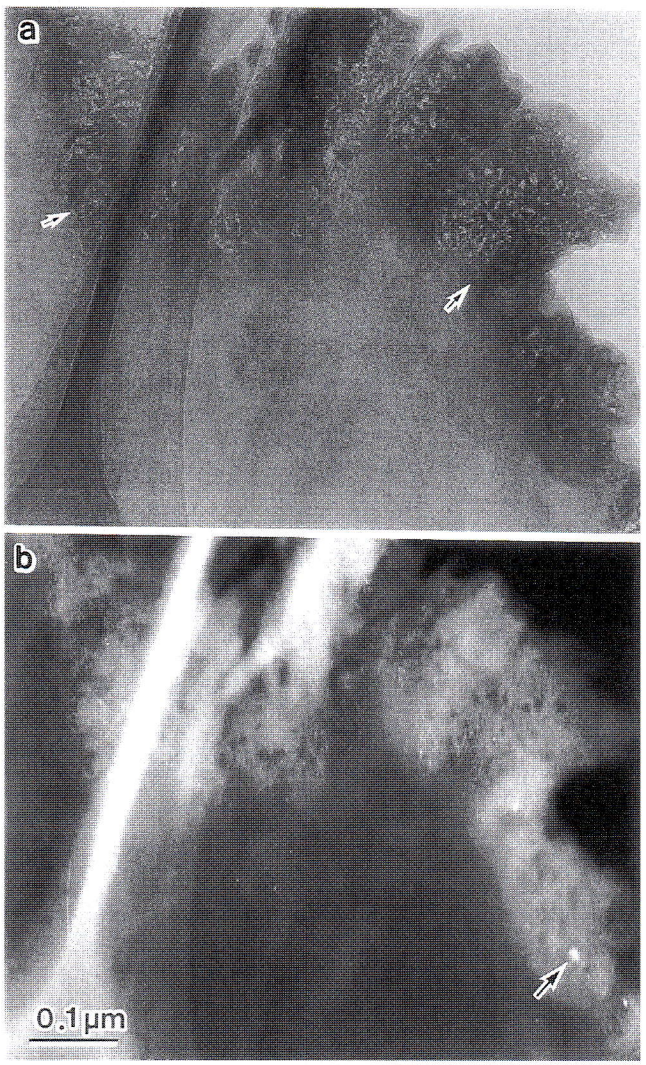

Figure 17: TEM images of an ultramicrotomed section of the chemical conversion coating film on AZ91D.
a: bright field image
b: dark field image

about 5 nm in size was locally found in a dark field image as shown in Fig.17 (b). This suggests that some of the film constituents tends to transform gradually to crystallites similarly to the anodic film.

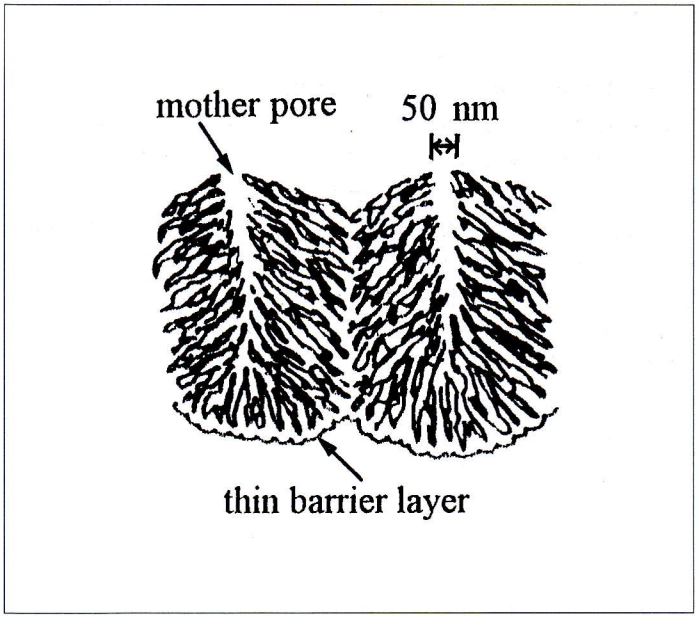

Figure 18: Schematic illustration of cell colonies of the chemical conversion coating film

X-ray diffraction analysis (14)

The analyzing depth estimated from the absorption coefficients of Cu Kα line for AZ91D alloy and pure magnesium is ca. 0.8 μm in the α-2θ mode where it was effectively independent of diffraction angle, and therefore the measurement in the α-2θ mode is much sensitive to the surface. On the other hand in the θ-2θ mode, it depends on 2θ and changes from 7 μm to 19 μm when 2θ is scanned from 35° to 100°. However, XRD patterns obtained in the α-2θ mode from the chemical conversion coated surface on pure Mg were identical as those of magnesium itself. For the coated surface on AZ91D, some of XRD peaks located close to those of MgF_2 and $NaMgF_3$, however, they were also corresponding to those of $Mg_{17}Al_{12}$(β phase) which presents at grain boundaries of the alloy. In spite of the small analyzing depth applied to the finished surfaces, the XRD patterns obtained were almost identical with those of the mechanically polished surface except intensity details caused by the difference in the angle scanning mode. It suggests that the surface films formed by chemical conversion coating in Dow 7 is effectively thin or of low density and contains no definite crystallites detectable by the XRD.

X-ray photo electron spectroscopy analysis (14)

Quantitative analysis was performed by considering the integrated spectral intensities and photo ionization cross sections. Components are identified from the electron binding energies and Auger parameters. The results indicate that the film contains large amounts of F^- and Mg^{2+}, medium amounts of 0^{2-} and OH^- and small amounts of Cr^{3+} and NH_4^+. Fair amounts of Na^+ and Al^{3+}, and small amounts of Fe^{3+} and Mn^{4+} are additionally found in the films formed on AZ91D (Table 5). Since MgO crystal is hardly found in the film, it is amorphous magnesium oxyhydroxide that is formed. In the cases of aluminum and iron, the formation of their oxyhydroxide on the individual substrate surface is well known. In the case of pure magnesium, the major film compositions are likely to be MgF_2, $MgO_x(OH)_y$, $NaMgF_3$, Cr_2O_3 and NH_4^+ as shown in Table 6. The film formed on AZ91D also contains $AlO_x(OH)_y$ and $FeO_x(OH)_y$ in addition to above compound. These are comparable with that detected in anodic films on pure magnesium (11). Atomic ratio of Al to Mg notably increases from 0.1 to 0.24 in the film compared with that in the AZ91D substrate alloy. Zn, which is included 1% in the AZ91D substrate is not detected in the film. The reason of low content of $NaMgF_3$ in the film on AZ91D may have been due to smaller film thickness caused by shorter formation time as discussed later and in the previous paper (11).

Table 5 - XPS quantitative analysis of the Dow 7 chemical conversion coated film formed on pure magnesium

Element	at%	Compound	mole %
Mg	22	MgF_2	27
Na	11	$NaMgF_3$	43
Cr	2.3	Cr_2O_3	4
F	45.5	-	-
N	2.2	NH_4^+	9
O	6	$MgO_x(OH)_y$	17
OH	11	-	-

Table 6 - XPS quantitative analysis of the Dow 7 chemical conversion coated film formed on magnesium die cast AZ91D

Element	at%	Compound	mole %
Mg	32	MgF_2	18
Na	0.42	$NaMgF_3$	1
Cr	25	Cr_2O_3	3
Al	7.5	$AlO_x(OH)_y$	16
Fe	1.6	$FeO_x(OH)_y$	4
Mn	0.06	-	-
F	33	-	-
N	3.4	NH_4^+	7
O	4.6	$MgO_x(OH)_y$	51
OH	15	-	-

Growth mechanism of chemical conversion coating films

Based on the above results, the following process of film growth by chemical conversion coating on magnesium and magnesium alloys can be deduced. Film growth proceeds mainly by the formation of MgF_2 and $MgO_x(OH)_y$ at the metal / film interface and the dissolution of the film at pore bases as an anodic process. The mobility of F^- across the barrier layer may be higher than that of O^{2-}. Some of film components such as MgF_2 tends to crystallize in the amorphous $MgO_x(OH)_y$ matrix to form small particles. $NaMgF_3$ is formed along with film growth in the outer part of the film by a chemical reaction under the presence of Na^+ in the electrolyte. Therefore, the content of $NaMgF_3$ is dependent on formation time. Dissolved Fe^{3+} precipitate in the film to form $FeO_x(OH)_y$. The formation and incorporation of Cr_2O_3 in the film can occur as a result of the reduction of Cr^{6+} to Cr^{3+} at the cathodic sites.

Since the grain boundary is composed of $Mg_{17}Al_{12}$ and is more noble than the matrix as reported by Lunder and Nisancioglu (24), it is supposed to be cathodic site. However, most of grain boundaries become hollow after the coating. This is partly due to original cavities between grains of the substrate. Further, $Mg_{17}Al_{12}$ could dissolve in the fluoride electrolyte at any rate since AlF_3, is more soluble than MgF_2, in a hot solution. It causes enrichment of Al by the precipitation of $AlO_x(OH)_y$ in the film.

CONCLUSIONS

Recent research development concerning surface phenomena and protective film growth on magnesium and magnesium alloys, which was mainly carried out by the author and coworkers, has been reviewed. Through the investigations on morphology and structure of naturally formed oxides on magnesium, it is confirmed that the thickness and composition, which are related to stability and passivity of the surface, are strongly affected by alloying elements. These advantages can be understood in terms of increased passivity of the metal surface by incorporation of components which stabilize the oxides. The increase in aluminum content, by enrichment of the Al_2O_3 component, is significant as the bulk composition of the alloy is increased above 4%, a threshold corresponding also to a significant improvement in corrosion resistance of these alloys. The Al/Mg weight ratio corresponding this transition is about 35%. Fundamental studies on thicker protective films grown by surface treatments such as anodizing and chemical conversion coating established that the films were essentially composed of anodically formed cylindrical porous oxides and barrier layer, which are similar to the Keller's model of anodic alumina. This type of information, obtained by direct TEM observation combined with surface analysis, must be very useful in attaining further success in the use of magnesium.

ACKNOWLEDGMENTS

The author is grateful to Prof. K. Nisancioglu, Dr. J.H. Nordlien, Prof. K. Asami and Prof. N. Masuko for their cooperation in this work and the helpful discussion. Parts of this work were financially supported by grant-in-aid for Scientific Research from Ministry of Education, Science, Sports and Culture, Japan and Iketani Science and Technology Foundation, and was performed under the inter- university cooperative research program of the Institute for Materials Research, Tohoku University.

REFERENCES

1) E.F. Emely, *Principles of Magnesium Technology,* Pergamon Press Ltd., New York (1966)
2) A. Niimi, Y. Itoi, and E. Sato, *J. Japan Inst. Light Metals* 30, 432 and 437 (1980).
3) M. Takaya, *J. Japan Inst. Light Metals* 37, 581 (1987).
4) F. Sato, Y. Asakawa, T. Nakayama, and H. Sato, *J. Japan Inst. Light Metals* 43, 65 (1993).
5) J.H. Nordlien, S. Ono, N. Masuko and K. Nisancioglu, *Corrosion Sci.,* 39, No.8, 1397- 1414 (1997)
6) J.H. Nordlien, S. Ono, N. Masuko and K. Nisancioglu, *J. Electrochem. Soc.,* 142, No.10, 3320-3322 (1995)
7) J.H. Nordlien, K. Nisancioglu, S. Ono and N. Masuko, *J. Electrochem. Soc.,* 143, No.8, 2564-2572 (1996)
8) J.H. Nordlien, K. Nisancioglu, S. Ono and N. Masuko, *J. Electrochem. Soc.,* 144, No.2, 461-466 (1997)
9) J.H. Nordlien, K. Nisancioglu, S. Ono and N. Masuko, *Proceedings of the 13th International Corrosion Conference,* Paper 258, 1-5 (Melbourne, Nov., 1996)
10) F. Keller, M. S. Hunter, and D. L. Robinson, *J. Electrochem. Soc.* 100, 411 (1953),
11) S. Ono, K. Asami, T. Osaka and N. Masuko, *J. Electrochemical Soc.,* 143, March, L62 (1996)
12) S. Ono, M.saito, M. Horiguchi, K. Terashima, K. Matsuzaka, A. Shida, T. Osaka, and N. Masuko, *J. Surf. Finish. Soc. Jpn,47,* 268 (1996).
13) S. Ono, M.saito, M. Horiguchi, K. Terashima, K. Matsuzaka, A. Shida, T. Osaka, and N. Masuko, *J. Surf. Finish. Soc. Jpn,* 47, 263 (1996).
14) S. Ono, K. Asami and T. Osaka, *Proceedings of the 13th International Corrosion Conference,* Paper 080 (Melbourne, Nov., 1996)
15) A. Shida, S. Ono, M.saito, M. Suzuki, M. Horiguchi, K. Terashima, K. Matsuzaka and N. Masuko, *J. Surf. Finish. Soc. Jpn,* 48, 349 (1997).
16) J. H. Nordlien, K. Nisancioglu, Abstract No.71, p.113, The Eletrochemical Society Meeting Abstracts, Vol.94-1, San Francisco, CA, May 22-27,1994.
17) N. Cabrera, N. F. Mott, Rep. Prog. Phys., 12, 163(1948-1949).
18) S. Ono, H. Ichinose, and N. Masuko, *Corros. Sci.* 33, 841(1992).
19) J. P. O'sallivan, and G. C. Wood, *Proc. Royal Soc. London* A317, 511 (1970).
20) P. M. Bradford, B. Case, G. Dearnaley, J. F. Turner, and I.S. Woolsey, *Corros. Sci.,* 16, 747 (1976).
21) E. Gulbrandsen, J. TaAo, and A. Olsen, *Corros. Sci.* 34, 1423 (1993).
22) K. Asami, K. Hashimoto, and S. Shimodaira, *Corros. Sci.,* 17, 713 (1977).
23) C. D. Wagner, L. H. Gale and R. H. Raymond, *Anal. Chem., 51,* 466 (1979).
24) O. Lunder, J. E. Lein, T. Kr.Aune and K. Nisancioglu, *Corrosion, 45,* 741 (1989).